Non-extensive statistical effects in high-energy collisions

EPJ manuscript No.
(will be inserted by the editor)

Non-extensive statistical effects in high-energy collisions

W.M. Alberico[1,3] and A. Lavagno[2,3]

[1] Dipartimento di Fisica, Università di Torino, Via P. Giuria 1, I-10124 Torino, Italy
[2] Dipartimento di Fisica, Politecnico di Torino, C.so Duca degli Abruzzi 24, I-10129 Torino, Italy
[3] Istituto Nazionale di Fisica Nucleare (INFN), Sezione di Torino, Italy

Received: date / Revised version: date

Abstract. Following the basic prescriptions of the relativistic Tsallis' non-extensive thermostatistics, we investigate from a phenomenological point of view the relevance of non-extensive statistical effects on relativistic heavy-ion collisions observable, such as rapidity spectra of net proton production, transverse momentum distributions and transverse momentum fluctuations. Moreover, we study the nuclear and the subnuclear equation of state, investigating the critical densities of a phase transition to a hadron-quark-gluon mixed phase by requiring the Gibbs conditions on the global conservation of the electric and the baryon charges. The relevance of small deviations from the standard extensive statistics is studied in the context of intermediate and high energy heavy-ion collisions.

PACS. 25.75.-q Relativistic heavy-ion collisions – 25.75.Nq Quark deconfinement, quark-gluon plasma production, and phase transitions – 05.90.+m Other topics in statistical physics, thermodynamics, and nonlinear dynamical systems

1 Introduction

It is common opinion that hadrons dissociate into a plasma of their elementary constituents, quarks and gluons (QGP), at density several times the nuclear matter density and/or at temperature above few hundreds MeV, which is the critical temperature T_c of the transition from the QGP phase to the hadronic gas phase and viceversa. Such a QGP is expected to have occurred in the early stages of the Universe and can be found in dense and hot stars, neutron stars, nucleus-nucleus high energy collisions where heavy ions are accelerated to relativistic energies [1]. After collision, a fireball is created which may realize the conditions of the QGP. The plasma then expands, cools, freezes-out into hadrons, photons, leptons that are detected and analyzed [2].

Since the interactions among quarks and gluons become weak at small distance or high energy, we could expect that QGP is a weakly interacting plasma, which can be described by perturbative QCD. However, this is rigorously true only at very high temperature ($T > T_c$) while at the order of the critical temperature and in the hadronization phase there are strong non-perturbative QCD effects.

In the literature, an ordinary plasma is usually characterized by the value of the plasma parameter Γ [3]

$$\Gamma = \frac{\langle U \rangle}{\langle T \rangle} \, , \tag{1}$$

defined as the ratio between potential energy $\langle U \rangle$ versus kinetic energy $\langle T \rangle$. When $\Gamma \ll 1$, one has a dilute weakly interacting gas; the Debye screening length λ_D is much greater than the average interparticle distance r_0 and a large number of particles is contained in the Debye sphere. Binary collisions induced by screened forces produce, in the classical case, the standard Maxwell-Boltzmann velocity distribution. If $\Gamma \approx 0.1 \div 1$, then $\lambda_D \approx r_0$, and it is not possible to clearly separate individual and collective degrees of freedom: this situation refers to a weakly interacting, non-ideal plasma. Finally, if $\Gamma \geq 1$, the plasma is strongly interacting, Coulomb interaction and quantum effects dominate and determine the structure of the system.

The quark-gluon plasma close to the critical temperature is a strongly interacting system. In fact, following Ref.[4,5], the color-Coulomb coupling parameter of the QGP is defined, in analogy with the one of the classical plasma, as

$$\Gamma \approx C \frac{g^2}{4\pi r_0 \, T} \, , \tag{2}$$

where $C = 4/3$ or 3 is the Casimir invariant for the quarks or gluons, respectively; for typical temperatures attained in relativistic heavy ion collisions, $T \simeq 200$ MeV, $\alpha_s = g^2/(4\pi) = 0.2 \div 0.5$, and $r_0 \simeq n^{-1/3} \simeq 0.5$ fm (n being the particle density for an ideal gas of 2 quark flavors in QGP). Consequently, one obtains $\Gamma \simeq 1.5 - 5$ and the plasma can be considered to be in a non-ideal liquid phase [5,6]. Furthermore, during the hadronization, non-perturbative, confining QCD effects are important, hence: i) near the critical temperature T_c, the effective quark mass is $m_q \approx T$

and $n < r >^3 \approx n\lambda_D^3 \simeq 1$; ii) the mean field approximation of the plasma is no longer correct and memory effects are not negligible.

In these conditions, the generated QGP does not satisfy anymore the basic assumptions (BBGKY hierarchy) of a kinetic equation (Boltzmann or Fokker-Planck equation) which describes a system toward the equilibrium. Indeed, near the phase transition the interaction range is much larger than the Debye screening length and a small number of partons is contained in the Debye sphere [4,6]. Therefore, the collision time is not much smaller than the mean time between collisions and the interaction is not local. The binary collisions approximation is not satisfied, memory effects and long–range color interactions give rise to the presence of non–Markovian processes in the kinetic equation, thus affecting the thermalization process toward equilibrium as well as the standard equilibrium distribution.

In the last years, there has been an increasing evidence that the generalized non-extensive statistical mechanics, proposed by Tsallis [7,8,9] and characterized by a power-law stationary particle distribution, can be considered as a basis for a theoretical framework appropriate to incorporate, at least to some extent and without going into microscopic dynamical description, long-range interactions, long-range microscopic memories and/or fractal space-time constraints. A considerable variety of physical issues show a quantitative agreement between experimental data and theoretical analyses based on Tsallis' thermostatistics. In particular, there is a growing interest to high energy physics applications of non-extensive statistics [10,11,12,13,14,15]. Several authors outline the possibility that experimental observations in relativistic heavy-ion collisions can reflect non-extensive statistical mechanics effects during the early stage of the collisions and the thermalization evolution of the system [4,16,17,18,19,20].

The aim of this paper is, in the light of the recent developments, to critically review our principal results obtained in the context of high energy heavy-ion collisions and to gain a new deeper insight on the nuclear equation of state and hadron-quark gluon mixed phase in the framework of non-extensive thermostatistics.

The paper is organized as follows. We start in Sec. II with a short reminder on the relativistic non-extensive thermodynamics. In Sec. III, we review the phenomenological studies on rapidity distribution of the net proton production; Sec. IV and in Sec. V are devoted to transverse observables by studying the transverse momentum distribution and the related transverse momentum fluctuations. In Sec. VI we investigate the effects of non-extensive thermostatistics on hadronic and quark-gluon equation of state; afterwards, we study the formation of hadron-quark mixed phase on the basis of the Gibbs condition in which both baryon and isospin charge are preserved.

2 Relativistic non-extensive thermodynamics

In order to study from a phenomenological point of view experimental observable in relativistic heavy-ion collisions, in this Section we present the basic macroscopic thermodynamic variables and kinetic theory in the language of the non-extensive relativistic kinetic theory.

Let us start by introducing the particle four-flow in the phase space as [21]

$$N^\mu(x) = \frac{1}{Z_q}\int \frac{d^3p}{p^0}\, p^\mu\, f(x,p)\ , \tag{3}$$

and the energy-momentum flow as

$$T^{\mu\nu}(x) = \frac{1}{Z_q}\int \frac{d^3p}{p^0}\, p^\mu p^\nu\, f^q(x,p)\ , \tag{4}$$

where we have set $\hbar = c = 1$, $x \equiv x^\mu = (t, \mathbf{x})$, $p \equiv p^\mu = (p^0, \mathbf{p})$, $p^0 = \sqrt{\mathbf{p}^2 + m^2}$ being the relativistic energy and $f(x,p)$ the particle distribution function. The four-vector $N^\mu = (n, \mathbf{j})$ represents the probability density $n = n(x)$ (which is normalized to unity) and the probability flow $\mathbf{j} = \mathbf{j}(x)$. The energy-momentum tensor contains the normalized q-mean expectation value of the energy density, as well as the energy flow, the momentum and the momentum flow per particle. Its expression follows directly from the definition of the mean q-expectation value in non-extensive statistics [8]; for this reason $T^{\mu\nu}$ it is given in terms of $f^q(x,p)$.

On the basis of the above definitions, one can show that it is possible to obtain a generalized non-linear relativistic Boltzmann equation [21]

$$p^\mu \partial_\mu \left[f(x,p)\right]^q = C_q(x,p)\ , \tag{5}$$

where the function $C_q(x,p)$ implicitly defines a generalized non-extensive collision term

$$C_q(x,p) = \frac{1}{2}\int \frac{d^3p_1}{p_1^0}\frac{d^3p'}{p'^0}\frac{d^3p'_1}{p'^0_1}\Big\{h_q[f',f'_1]W(p',p'_1|p,p_1) - h_q[f,f_1]W(p,p_1|p',p'_1)\Big\}\ . \tag{6}$$

Here $W(p,p_1|p',p'_1)$ is the transition rate between a two-particle state with initial four-momenta p and p_1 and a final state with four-momenta p' and p'_1; $h_q[f,f_1]$ is the q-correlation function relative to two particles in the same space-time position but with different four-momenta p and p_1, respectively. Such a transport equation conserves the probability normalization (number of particles) and is consistent with the energy-momentum conservation laws in the framework of the normalized q-mean expectation value. Moreover, the collision term contains a generalized expression of the molecular chaos and for $q > 0$ implies the validity of a generalized H-theorem, if the following, non-extensive, local four-density entropy is assumed (henceforward we shall set Boltzmann constant k_B to unity)

$$S_q^\mu(x) = -\int \frac{d^3p}{p^0}\, p^\mu f[(x,p)]^q[\ln_q f(x,p) - 1]\ , \tag{7}$$

where we have used the definition $\ln_q x = (x^{1-q} - 1)/(1-q)$, the inverse function of the Tsallis' q-exponential function

$$e_q(x) = [1 + (1-q)x]^{1/(1-q)}\ , \tag{8}$$

which satisfies the property $e_q(\ln_q x) = x$.

The above expression is written in a covariant form, in fact $S_q^\mu = (S_q^0, S_q^i)$, with $i = 1, 2, 3$, correctly transforms as a four-vector under Lorentz transformations [21], where S_q^0 is the standard expression of the Tsallis non-extensive local entropy density and S_q^i is the Tsallis entropy flow. Note that for $q \to 1$, Eq.(7) reduces to the well known four-flow entropy expression [22].

At equilibrium, the solution of the above Boltzmann equation is a relativistic Tsallis-like (power law) distribution and can be written as

$$f_{eq}(p) = \frac{1}{Z_q}\left[1 - (1-q)\frac{p^\mu U_\mu}{T}\right]^{1/(1-q)} , \qquad (9)$$

where U_μ is the hydrodynamic four-velocity [22] and f_{eq} depends only on the momentum in the absence of an external field. At this stage, T is a free parameter and only in the derivation of the equation of state it will be identified with the physical temperature.

We are able now to evaluate explicitly all other thermodynamic variables and provide a complete macroscopic description of a relativistic system at the equilibrium. Considering the decomposition of the energy-momentum tensor: $T^{\mu\nu} = \epsilon\, U^\mu U^\nu - P\, \Delta^{\mu\nu}$, where ϵ is the energy density, P the pressure and $\Delta^{\mu\nu} = g^{\mu\nu} - U^\mu U^\nu$, the equilibrium pressure can be calculated as

$$P = -\frac{1}{3} T^{\mu\nu}\Delta_{\mu\nu} = -\frac{1}{3\, Z_q}\int \frac{d^3p}{p^0} p^\mu p^\nu \Delta_{\mu\nu} f_{eq}^q(p) . \qquad (10)$$

Setting $\tau = p^0/T$ and $z = m/T$, the above integral can be expressed as

$$P = \frac{4\pi}{Z_q}\, m^2\, T^2\, K_2(q, z) , \qquad (11)$$

where we have introduced the q-modified Bessel function of the second kind as follows

$$K_n(q, z) = \frac{2^n n!}{(2n)!}\frac{1}{z^n}\int_z^\infty d\tau (\tau^2 - z^2)^{n-1/2}\, \left(e_q^{-\tau}\right)^q , \qquad (12)$$

and $e_q(x)$ is the q-modified exponential defined in Eq.(8).

Similarly, the energy density ϵ can be obtained from the following expression

$$\epsilon = T^{\mu\nu} U_\mu U_\nu = \frac{1}{Z_q}\int \frac{d^3p}{p^0} (p^\mu U_\mu)^2 f_{eq}^q(p) , \qquad (13)$$

and, after performing the integration, it can be cast into the compact expression:

$$\epsilon = \frac{4\pi}{Z_q}\, m^4 \left[3\frac{K_2(q, z)}{z^2} + \frac{K_1(q, z)}{z}\right] . \qquad (14)$$

Thus the energy per particle $e = \epsilon/n$ is

$$e = 3\, T + m\, \frac{K_1(q, z)}{K_2(q, z)} , \qquad (15)$$

which has the same structure of the relativistic expression obtained in the framework of the equilibrium Boltzmann-Gibbs statistics [22].

It is also interesting to consider the ratio ϵ/p, a quantity often considered in lattice calculations as an indicator for the phase transition [23]:

$$\frac{\epsilon}{P} = 3\left(1 + \frac{z}{3}\frac{K_1(q, z)}{K_2(q, z)}\right) , \qquad (16)$$

which tends to the Stefan-Boltzmann limit 3 in the limit of very large temperatures.

In the non-relativistic limit ($p \ll 1$) the energy per particle reduces to the well-known expression

$$e \simeq m + \frac{3}{2}\, T , \qquad (17)$$

and no explicit q-dependence is left over.

Hence from the above results it appears that, in searching for the relevance of non-extensive statistical effects, both microscopic observable, such as particle distribution, correlation functions, fluctuations of thermodynamical variables, and macroscopic variables, such as energy density or pressure, can be affected by the deformation parameter q.

In this context, it appears relevant to observe that, in Ref. [15] non-extensive Boltzmann equation has been studied and proposed for describing the hadronization of quark matter. Moreover, starting from the above generalized relativistic kinetic equations, in Ref.[19] the authors have recently formulated a non-extensive hydrodynamic model for multiparticle production processes in relativistic heavy-ion collisions. These works represent an important bridge for a close connection between a microscopic non-extensive model and experimental observable.

Finally, let us remind the reader that for a system of particles in a degenerate regime the above classical distribution function (9) has to be modified by including the fermion and boson quantum statistical prescriptions. For a dilute gas of particles and/or for small deviations from the standard extensive statistics ($q \approx 1$) the equilibrium distribution function, in the grand canonical ensemble, can be written as [24]

$$n^q(k, \mu) = \frac{1}{[1 + (q-1)(E(k) - \mu)/T]^{1/(q-1)} \pm 1} , \qquad (18)$$

where the sign + stands for fermions and − for bosons: hence all previous results can be easily extended to the case of quantum statistical mechanics.

3 Rapidity distributions

Recent results for net-proton rapidity spectra in central Au+Au collisions at the highest RHIC energy of $\sqrt{s_{NN}}$= 200 GeV [25] show an unexpectedly large rapidity density at midrapidity in comparison with analogous spectra at lower energy at SPS [26] and AGS [27]. As outlined from

different authors, such spectra can reflect non-equilibrium effects even if the energy dependence of the rapidity spectra is not very well understood [25,28].

In this Section we are going to discuss from a phenomenological point of view the relevance of non-extensive statistical mechanics and anomalous diffusion in a power law Fokker-Planck kinetic equation which describes the non-equilibrium evolution of the rapidity spectra of net proton yield. Let us recall, in this context, that similar approaches have been considered in the past to analyze transverse momentum distributions, power law spectra at large $p_\perp$ and two-particle Bose-Einstein correlation functions in terms of various non-conventional extensions of the Boltzmann-Gibbs thermostatistics [16,18,29]. Relevant results have been also obtained by Wolschin [30,31,32] within a three-component relativistic diffusion model.

In order to study the rapidity spectra, it is convenient to separate the kinetic variables into their transverse and longitudinal components, the latter being related to the rapidity $y = \tanh^{-1}\left(p_\parallel/\sqrt{m^2+p^2}\right)$. If we assume that the particle distribution function $f(y, m_\perp, t)$, at fixed transverse mass $m_\perp = \sqrt{m^2+p_\perp^2}$, is not appreciably influenced by the transverse dynamics (which is considered in thermal equilibrium), the non-linear Fokker-Planck equation in the rapidity space y can be written as [33]

$$\frac{\partial}{\partial t}[f(y,m_\perp,t)] = \frac{\partial}{\partial y}\Big[J(y,m_\perp)[f(y,m_\perp,t)] + D\frac{\partial}{\partial y}[f(y,m_\perp,t)]^\mu\Big] , \qquad (19)$$

where D and J are the diffusion and drift coefficients, respectively, while μ is a generic, real exponent.

Tsallis and Bukman [34] have shown that, for linear drift, the time dependent solution of the above equation is a Tsallis distribution with $\mu = 2-q$ and that a value of $q \neq 1$ implies anomalous diffusion, i.e., $[y(t) - y_M(t)]^2$ scales like t^α, with $\alpha = 2/(3-q)$. For $q < 1$, the above equation implies anomalous sub-diffusion, while for $q > 1$, we have a super-diffusion process in the rapidity space. Let us observe that, at variance with our approach, if one assumes a Fokker-Planck equation with fractional derivatives, in the framework of the so-called continuous time random (Lévy) walk models, anomalous diffusion processes can be also realized [35,36,37].

Let us observe that the choice of the diffusion and the drift coefficients plays a crucial rôle in the solution of the above non-linear Fokker-Planck equation (19). Such a choice influences the time evolution of the system and its equilibrium distribution. By imposing the validity of the Einstein relation for Brownian particles, we can generalize to the relativistic case the standard expressions of diffusion and drift coefficients as follows

$$D = \gamma\, T\ , \qquad J(y,m_\perp) = \gamma\, m_\perp \sinh(y) \equiv \gamma\, p_\parallel\ , \qquad (20)$$

where $p_\parallel$ is the longitudinal momentum, T is the temperature and γ is a common constant. Let us remark that the above definition of the diffusion and drift coefficients appears as the natural generalization to the relativistic Brownian case in the rapidity space. The drift coefficient which is linear in the longitudinal momentum $p_\parallel$ becomes non-linear in the rapidity coordinate.

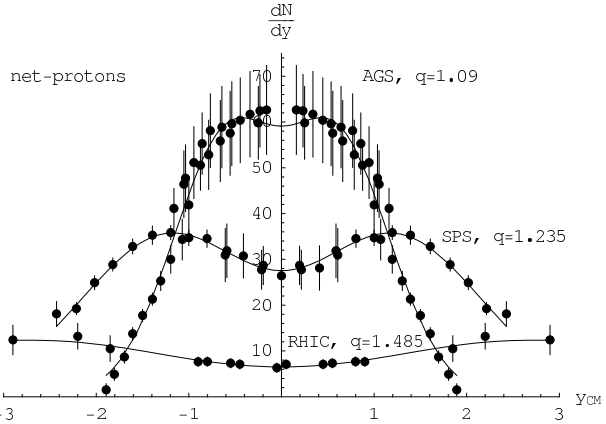

Fig. 1. Rapidity spectra for net proton production ($p-\overline{p}$) at RHIC (Au+Au at $\sqrt{s_{NN}} = 200$ GeV, BRAHMS data), SPS (Pb+Pb at $\sqrt{s_{NN}} = 17.3$ GeV, NA49 data) and AGS (Au+Au at $\sqrt{s_{NN}} = 5$ GeV, E802, E877, E917).

It is easy to see that the above coefficients give us the Boltzmann stationary distribution in the linear case ($q = \mu = 1$), while the equilibrium solution $f^{eq}(y, m_\perp)$ of Eq.(19), with $\mu = 2-q$, is a Tsallis-like (power-law) distribution with the relativistic energy $E = m_\perp \cosh(y)$

$$f^{eq}(y,m_\perp) \propto \Big[1-(1-q)\, m_\perp \cosh(y)/T\Big]^{1/(1-q)} . \qquad (21)$$

The rapidity distribution at fixed time can be obtained out of equilibrium by means of numerical integration of Eq.(19) with delta function initial conditions depending upon the value of the experimental projectile rapidities and by means of numerical integration over the transverse mass $m_\perp$

$$\frac{dN}{dy}(y,t) = c\int_m^\infty m_\perp^2\ \cosh(y)\, f(y,m_\perp,t)\, dm_\perp\ , \qquad (22)$$

where m is the mass of the considered particles and c is a normalization constant, fixed by comparison with the experimental data. The calculated rapidity spectra will ultimately depend on two parameters: the "interaction" time $\tau_{int} = m\,\gamma\, t$ and the non-extensive parameter q.

It is important to note that, as we will see in the next Section by studying the transverse mass spectrum, dynamical collective interactions are intrinsically involved in the generalized non-extensive statistical mechanics and, in a purely thermal source, a generalized q-blue shift factor (strictly related to the presence of longitudinal flow) appears. In this context, it is worth mentioning that collective transverse flow effects in the framework of a non-extensive statistical mechanics have been investigated in Ref. [16] as well.

In Fig. 1, we report the rapidity distribution obtained from Eq. (22) (full line) for the net proton production

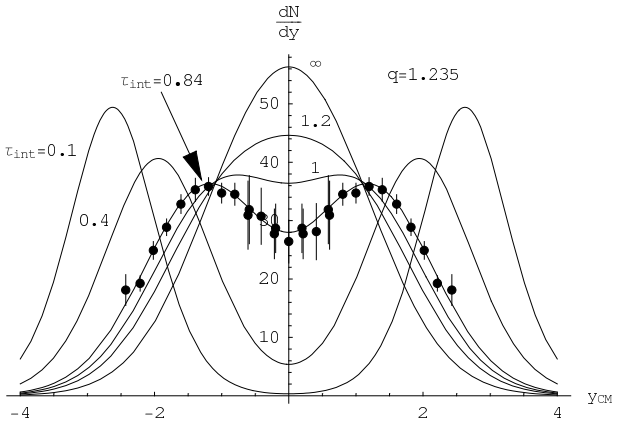

Fig. 2. Time evolution of the rapidity spectra at fixed value of $q = 1.235$, obtained for SPS data. The data can be well reproduced only for this value of q and for the corresponding value of $\tau_{int} = 0.84$.

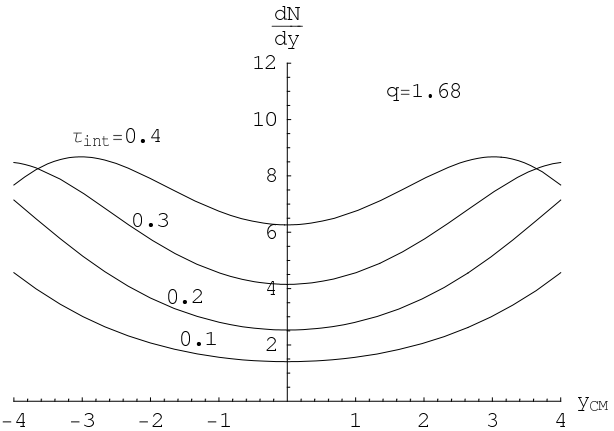

Fig. 3. Rapidity spectra for net proton production expected at LHC for the extrapolated value of $q = 1.68$ and different interaction times τ_{int}.

$(p - \overline{p})$ compared with the experimental data of RHIC (Au+Au at $\sqrt{s_{NN}} = 200$ GeV, [25]), SPS (Pb+Pb at $\sqrt{s_{NN}} = 17.3$ GeV, [26]) and AGS (Au+Au at $\sqrt{s_{NN}} = 5$ GeV, [27]). The parameters employed for the three curves are: $q = 1.485$ with $\tau_{int} = 0.47$ for RHIC, $q = 1.235$ with $\tau_{int} = 0.84$ for SPS and $q = 1.09$ with $\tau_{int} = 0.95$ for AGS, respectively. Let us notice that the value $\tau_{int} = 0.47$ is compatible with the equilibration time extracted from a hydro-description of the RHIC data: this partly justifies the present use of near-equilibrium distributions.

We also remark that, although q and τ_{int} appear, in principle, as independent parameters, in fitting the data they are not. We can see that in the non-linear case only $(q \neq 1)$ there exists indeed one (and only one) finite time τ_{int} for which the obtained rapidity spectrum well reproduces the broad experimental shape. On the contrary, for $q = 1$, no value of τ_{int} can be found, which allows to reproduce the data. Evidence for this feature is shown in Fig. 2, where the time evolution of the rapidity spectra is reported at the fixed value $q = 1.235$, the one employed for the SPS experiment, and different values of τ_{int}: only for $\tau_{int} = 0.84$ a good agreement with the experimental data is obtained. Moreover, for different values of q we do not find a corresponding value of the τ_{int} parameter which allows us to reproduce the selected data.

We obtain a remarkable agreement with the experimental data by increasing the value of the non-linear deformation parameter q as the beam energy increases. At AGS energy, the non-extensive statistical effects are negligible and the spectrum is well reproduced within the standard quasi-equilibrium linear approach. At SPS energy, non-equilibrium effects and non-linear evolution become remarkable ($q = 1.235$) and such effects are even more evident for the very broad RHIC spectra ($q = 1.485$).

From a phenomenological point of view, we can interpret the larger value of the parameter q and the shorter τ_{int} needed to fit the RHIC data, as a signal of non-linear anomalous (super) diffusion. As confirmed by recent microscopic calculations [5,6], strongly coupled non-ideal plasma is generated at energy densities corresponding to the order of the critical phase transition temperature and in such a regime we find, in our macroscopic approach, strong deviations from the standard thermostatistics. At much higher energy, such as the LHC (Large Hadron Collider - CERN Laboratory) one, we can foresee a minor relevance of such non-ideal effects since the considerable expected energy density is far above the critical one. Nevertheless we can guess, on the basis of a linear extrapolation of the q-value versus the beam rapidity, that a suitable q-value for LHC will be $q = 1.68$. Accordingly we show in Fig. 3 the expected net-proton distributions, evaluated at different $\tau_{int} \leq 0.4$.

4 Transverse momentum distributions

High transverse momentum particle production in hadronic collisions results from the fragmentation of quarks and gluons emerging from the initial scattering at large Q^2, therefore, hard processes in nucleus-nucleus collisions provide direct information on the early partonic phases of the reaction and particle production at high transverse momentum is sensitive to properties of the hot and dense matter in the nuclear collisions. For this reason and for the motivations reported in the Introduction, we expect that the transverse momentum spectra will be sensibly affected by non-extensive statistical effects.

The single particle spectrum can be expressed as an integral over a freeze–out hypersurface Σ_f

$$E\frac{d^3N}{d^3p} = \frac{dN}{dy\, m_\perp dm_\perp d\phi} = \frac{g}{(2\pi)^3}\int_{\Sigma_f} p^\mu d\sigma_\mu(x) f(x,p)\,, \tag{23}$$

where g is the degeneracy factor and $f(x,p)$ is the phase–space distribution.

The transverse momentum distribution depends on the phase-space distribution and usually an exponential shape is employed to fit the experimental data. This shape is obtained by assuming a purely thermal source with a Boltzmann distribution and the transverse momentum spec-

trum can be expressed as

$$\frac{dN}{m_\perp dm_\perp} = A\, m_\perp K_1\,(z)\ , \qquad (24)$$

where $z = m_\perp/T$, $m_\perp = \sqrt{p_\perp^2 + m^2}$, and K_1 is the first order modified Bessel function. In the asymptotic limit, $m_\perp \gg T$ ($z \gg 1$), the above expression gives rise to the exponential shape

$$\frac{dN}{m_\perp dm_\perp} = B\,\sqrt{m_\perp}\, e^{-z}\ . \qquad (25)$$

High energy deviations from the exponential shape can be taken into account by introducing a dynamical effect due to collective transverse flow, also called blue-shift, with an increase of the slope parameter T at large $m_\perp$.

Let us consider a different point of view and argue that the deviation from the Boltzmann slope at high $p_\perp$ can be ascribed to the presence of non-extensive statistical effects in the steady state distribution of the particle gas. In this framework, at the first order in $(q-1)$ the transverse mass spectrum can be written as [4]

$$\frac{dN}{m_\perp dm_\perp} = C\, m_\perp \Big\{ K_1\,(z) + \frac{(q-1)}{8} z^2\,[3\,K_1(z) + K_3(z)] \Big\}\ , \qquad (26)$$

where K_3 is the modified Bessel function of the third order. In the asymptotic limit, $z \gg 1$, we have

$$\frac{dN}{m_\perp dm_\perp} = D\,\sqrt{m_\perp}\,\exp\left(-z + \frac{q-1}{2}\,z^2\right)\ , \qquad (27)$$

and we may obtain the generalized slope parameter or q-blue shift (if $q > 1$)

$$T_q = T + (q-1)\, m_\perp\ . \qquad (28)$$

Let us notice that the slope parameter depends on the detected particle mass and it increases with the energy (if $q > 1$) as it was observed in the experimental results [38].

In the same manner, the particle invariant yield at midrapidity, for central collisions and in the framework of non-extensive statistics, can be written in terms of the equilibrium Tsallis-like distribution (9) as

$$\frac{d^2N}{2\pi p_\perp dp_\perp dy} = C\, m_\perp \left[1 - (1-q)\frac{m_\perp}{T}\right]^{1/(1-q)}\ , \qquad (29)$$

where C is a normalization constant.
In Fig. 4, we report the experimental neutral pion invariant yields in central Pb+Pb collisions at $\sqrt{s_{NN}}$=17.3 GeV (SPS) [39] and in central Au+Au collisions at $\sqrt{s_{NN}}$=200 GeV (RHIC) [40] compared with the modified non-extensive thermal distribution shape of Eq.(29). For Pb+Pb collisions we have set the non-extensive parameter $q = 1.038$ with T=140 MeV and for Au+Au collisions $q = 1.07$ with T=160 MeV. It is important to outline that, for consistency, the same value extracted in the central Pb+Pb collisions will be used in the next Section in the evaluation

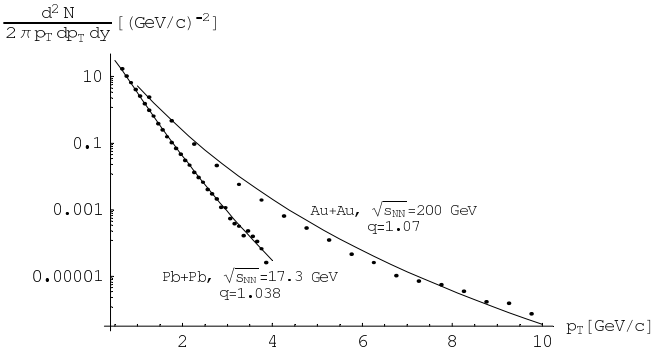

Fig. 4. Experimental neutral pion invariant yields in central Pb+Pb collisions at $\sqrt{s_{NN}}$=17.3 GeV [39] and in central Au+Au collisions at $\sqrt{s_{NN}}$=200 GeV [40] compared with the modified thermal distribution shape by using non-extensive statistics ($q = 1.038$ for Pb+Pb and $q = 1.07$ for Au+Au collisions.)

of the transverse momentum fluctuations at the same SPS energy. Similar results have been obtained by reproducing the experimental $S+S$ transverse momentum distribution (NA35 data [41]) in Ref. [4] and, always in the framework of non–extensive statistics, in Ref.[10].

Let us observe that the values of the entropic q-parameter, used in the fit of the transverse momentum distributions, are sensibly smaller than the ones extracted from the rapidity spectra of the previous Section. The reason of this remarkable difference lies in the completely different nature of the transverse and longitudinal observables. It is rather common opinion that the longitudinal rapidity distribution is not appreciably influenced by the transverse dynamics, which is considered in thermal equilibrium. The other way round, rapidity spectra is affected by non-equilibrium features and the dynamics of the interactions, strongly related to the value of the q-parameter in our macroscopic phenomenological approach, results sensibly different.

5 Transverse momentum fluctuations

Gaździcki and Mrówczyński introduced the following quantity [42,43]

$$\Phi_{p_\perp} = \sqrt{\frac{\langle Z_{p_\perp}^2\rangle}{\langle N\rangle}} - \sqrt{\overline{z_{p_\perp}^2}}\ , \qquad (30)$$

where $z_{p_\perp} = p_\perp - \overline{p}_\perp$ and $Z_{p_\perp} = \sum_{i=1}^{N}(p_{\perp i} - \overline{p}_{\perp i})$, N is the multiplicity of particles produced in a single event. Non-vanishing Φ implies effective correlations among particles which alter the momentum distribution.

In the framework of non–extensive statistics and keeping in mind that it preserves the whole mathematical structure of the thermodynamical relations, it is easy to show that the two terms in the right hand side of Eq.(30) can be expressed in the following simple form

$$\overline{z_{p_\perp}^2} = \frac{1}{\rho}\int \frac{d^3p}{(2\pi)^3}\,\Big(p_\perp - \overline{p}_\perp\Big)^2\,\langle n\rangle_q\ , \qquad (31)$$

and

$$\frac{\langle Z^2_{p_\perp}\rangle}{\langle N\rangle} = \frac{1}{\rho}\int \frac{d^3p}{(2\pi)^3}\left(p_\perp - \overline{p}_\perp\right)^2 \langle \Delta n^2\rangle_q \,, \qquad (32)$$

where

$$\overline{p}_\perp = \frac{1}{\rho}\int \frac{d^3p}{(2\pi)^3}\, p_\perp \langle n\rangle_q \qquad (33)$$

with

$$\rho = \int \frac{d^3p}{(2\pi)^3}\langle n\rangle_q \,. \qquad (34)$$

In the above equations we have indicated with $\langle n\rangle_q$ the following mean occupation number of bosons [24]

$$\langle n\rangle_q = \frac{1}{[1+(q-1)\beta(E-\mu)]^{1/(q-1)}-1} \,, \qquad (35)$$

and with $\langle \Delta n^2\rangle_q = \langle n^2\rangle_q - \langle n\rangle_q^2$ the generalized particle fluctuations, given by

$$\langle \Delta n^2\rangle_q \equiv \frac{1}{\beta}\frac{\partial\langle n\rangle_q}{\partial\mu} = \frac{\langle n\rangle_q}{1+(q-1)\beta(E-\mu)}\left(1\mp\langle n\rangle_q\right)$$
$$= \langle n\rangle_q^q\,\left(1\mp\langle n\rangle_q\right)^{2-q}. \qquad (36)$$

NA49 Collaboration has measured the correlation $\Phi_{p_\perp}$ of the pion transverse momentum (Pb+Pb at 158 A GeV) [44] obtaining $\Phi^{exp}_{p_\perp} = (0.6\pm1)$ MeV. This value is the sum of two contributions: $\Phi^{st}_{p_\perp} = (5\pm1.5)$ MeV, the measure of the statistical two-particle correlation, and $\Phi^{tt}_{p_\perp} = (-4\pm 0.5)$ MeV, the anti-correlation from limitation in two-track resolution.

Standard statistical calculations ($q=1$) give [43] $\Phi^{st}_{p_\perp} =$ 24.7 MeV at $T = 170$ MeV, $\mu = 60$ MeV. In the frame of non–extensive statistics, for $q = 1.038$ (for consistency, the same value extracted in the previous Section from neutral pion invariant yield for central Pb+Pb collisions at the same energy in consideration), we obtain the experimental (statistical) value: $\Phi^{st}_{p_\perp} = 5$ MeV at $T = 170$ MeV and $\mu = 60$ MeV.

In Fig. 5, we show the partial contributions to the quantity $\Phi_{p_\perp}$, by using Eq.s (31) and (32), and by extending the integration over $p_\perp$ to partial intervals $\Delta p_\perp =$ 0.5 GeV at $T = 170$ MeV and $\mu = 60$ MeV. In the standard statistics (dashed line), $\Phi_{p_\perp}$ is always positive and vanishes in the $p_\perp$-intervals above ≈ 1 GeV. In the non-extensive statistics (solid line), instead, the fluctuation measure $\Phi_{p_\perp}$ becomes negative for $p_\perp$ larger than 0.5 GeV and becomes vanishingly small only in $p_\perp$-intervals above ~ 3 GeV. If measured in separate $p_\perp$ bins, such a negative value of $\Phi_{p_\perp}$ at high $p_\perp$ could be an evidence of the presence of non-extensive regime in heavy-ions collisions.

Finally, in this context it is important to outline that a critical overview of the $\Phi_{p_\perp}$ measure of fluctuations and correlations was given in Ref.s [45,46]. It was shown that $\Phi_{p_\perp}$ measure is very sensitive to the constraints provided by the energy-momentum conservation laws and to the effects of correlations. These effects should be carefully accounted in the phenomenological studies related to event by event analysis of data.

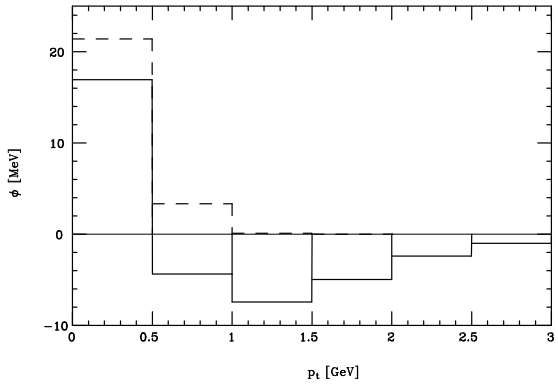

Fig. 5. The partial contributions to the correlation measure $\Phi_{p_\perp}$ [MeV] in different $p_\perp$ intervals. The dashed line refers to standard statistical calculations with $q = 1$, the solid line corresponds to $q = 1.038$.

6 Non-extensive nuclear equation of state

As partially discussed in the Introduction, hadronic matter is expected to undergo a phase transition into a deconfined phase of quarks and gluons at large densities and/or high temperatures. However, the extraction of experimental information about the Equation of State (EOS) of matter at large densities and temperatures from the data of intermediate and high energy heavy-ion collisions is very complicated. Possible indirect indications of a softening of the EOS at the energies reached at AGS have been discussed several times in the literature [47,48]. In particular, a recent analysis [49] based on a 3-fluid dynamics simulation suggests a progressive softening of the EOS tested through heavy-ion collisions at energies ranging from 2A GeV up to 8A GeV. On the other hand, the information coming from experiments with heavy-ions at intermediate and high energy collisions is that, for symmetric or nearly symmetric nuclear matter, the critical density (at low temperatures) appears to be considerably larger than nuclear matter saturation density ρ_0. Concerning non-symmetric matter, general arguments based on Pauli principle suggest that the critical density decreases with Z/A. Therefore, the transition's critical densities are expected to sensibly depend on the isospin of the system [50]. Moreover, the analysis of observations of neutron stars, which are composed of β-stable matter for which $Z/A \leq 0.1$, can also provide hints on the structure of extremely asymmetric matter at high density. No data on the quark deconfinement transition are at the moment available for intermediate values of Z/A. Recently, it has been proposed by several groups to produce unstable neutron-rich beams at intermediate energies. These new experiments can open the possibility to explore in laboratory the isospin dependence of the critical densities.

The aim of this Section is to study the behavior of the nuclear equation of state at finite temperature and baryon density and to explore the existence of a hadron-quark mixed phase at a fixed value of Z/A. Furthermore, from the above considerations, it appears reasonable that

in regime of high density and temperature both hadron and quark-gluon EOS can be sensibly affected by non-extensive statistical effects [51]. The relevance of these effects on the relativistic hadronic equation of state has also been recently point out in Ref. [52].

The scenario we are going to explore in this last Section corresponds to the situation realized in experiments at not too high energy. In this condition, only a small fraction of strangeness can be produced and, therefore, we limit ourselves to study the deconfinement transition from nucleonic matter into up and down quark matter. In the next two subsections, we will study the two corresponding EOSs separately, on the basis on the previously reported non-extensive relativistic thermodynamic relations. The existence of the hadron-quark mixed phase will be studied in the third subsection. This investigation may be helpful also in view of the future experiments planned, e.g., at the facility FAIR at GSI [53].

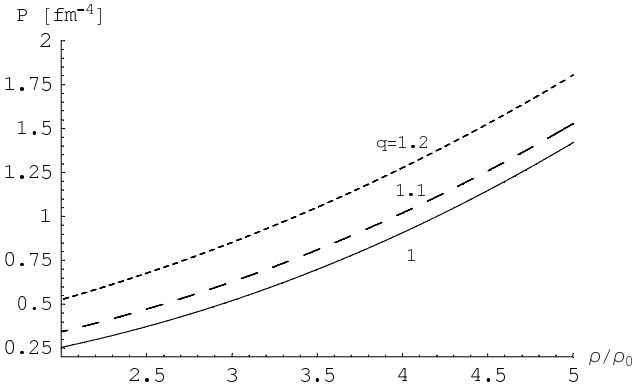

Fig. 6. Hadronic equation of state: pressure versus baryon number density (in units of the nuclear saturation density ρ_0) for different values of q. In the figure $T = 100$ MeV and $Z/A = 0.4$.

6.1 Non-extensive hadronic equation of state

Concerning the hadronic phase, we use a relativistic self-consistent theory of nuclear matter in which nucleons interact through the nuclear force mediated by the exchange of virtual isoscalar and isovector mesons (σ, ω, ρ) [54]. On the basis of the Eqs.(4), (10) and (13), the pressure and the energy density can be written as

$$P = \sum_{i=n,p} \frac{2}{3} \int \frac{\mathrm{d}^3k}{(2\pi)^3} \frac{k^2}{E_i^\star(k)} [n_i^q(k,\mu_i^\star) + n_i^q(k,-\mu_i^\star)] - \frac{1}{2}m_\sigma^2\sigma^2 - \frac{1}{3}a\sigma^3 - \frac{1}{4}b\sigma^4 + \frac{1}{2}m_\omega^2\omega_0^2 + \frac{1}{2}m_\rho^2\rho_0^2, \quad (37)$$

$$\epsilon = \sum_{i=n,p} 2 \int \frac{\mathrm{d}^3k}{(2\pi)^3} E_i^\star(k) [n_i^q(k,\mu_i^\star) + n_i^q(k,-\mu_i^\star)] + \frac{1}{2}m_\sigma^2\sigma^2 + \frac{1}{3}a\sigma^3 + \frac{1}{4}b\sigma^4 + \frac{1}{2}m_\omega^2\omega_0^2 + \frac{1}{2}m_\rho^2\rho_0^2, \quad (38)$$

where $n_i(k,\mu_i)$ and $n_i(k,-\mu_i)$ are the fermion particle and antiparticle distribution (18). The nucleon effective energy is defined as $E_i^\star = \sqrt{k^2 + {M_i^\star}^2}$, where $M_i^\star = M_i - g_\sigma\sigma$. The effective chemical potentials $\mu_i^\star$ are given in terms of the vector meson mean fields $\mu_i^\star = \mu_i - g_\omega\omega_0 \mp g_\rho\rho_0$ ($-$ proton, $+$ neutron), where μ_i are the thermodynamical chemical potentials $\mu_i = \partial\epsilon/\partial\rho_i$. At zero temperature they reduce to the Fermi energies $\mu_i^\star = E_{Fi}^\star \equiv \sqrt{k_{Fi}^2 + {M_i^\star}^2}$ and the non-extensive statistical effects disappear. The isoscalar and isovector meson fields (σ, ω and ρ) are obtained as a solution of the field equations in mean field approximation and the related couplings (g_σ, g_ω and g_ρ) are the free parameter of the model [54]. Finally, The baryon density ρ_B is given by

$$\rho_B = 2 \sum_{i=n,p} \int \frac{\mathrm{d}^3k}{(2\pi)^3} [n_i(k,\mu_i^\star) - n_i(k,-\mu_i^\star)]\,. \quad (39)$$

Note that statistical mechanics enters as an external ingredient in the functional form of the "free" particle distribution of Eq. (18). Since all the equations must be solved in a self-consistent way, the presence of non-extensive statistical effects in the particle distribution function influences the many-body interaction in the mean field self-consistent solutions obtained for the meson fields.

In Fig. 6, we report the resulting hadronic EOS: pressure as a function of the baryon number density for different values of q. Since in the previous Sections we have phenomenologically obtained values of q greater than unity, we will concentrate our analysis to $q > 1$. The results are plotted at the temperature $T = 100$ MeV, at fixed value of $Z/A = 0.4$ and we have used the GM2 set of parameters of Ref.[54]. The range of the considered baryon density and the chosen values of the parameters correspond to a physical situation which can be realized in the recently proposed high energy heavy-ion collisions experiment at GSI [55].

6.2 Non-extensive QGP equation of state

In the simple model of free quarks in a bag [56], the pressure, energy density and baryon number density for a relativistic Fermi gas of quarks in the framework of non-extensive statistics (see Eqs.(3), (4), (10) and (13)) can be written, respectively, as

$$P = \sum_{f=u,d} \frac{1}{3} \frac{\gamma_f}{2\pi^2} \int_0^\infty k \frac{\partial\epsilon_f}{\partial k} [n_f^q(k,\mu_f) + n_f^q(k,-\mu_f)] k^2 dk - B, \quad (40)$$

$$\epsilon = \sum_{f=u,d} \frac{\gamma_f}{2\pi^2} \int_0^\infty \epsilon_f [n_f^q(k,\mu_f) + n_f^q(k,-\mu_f)] k^2 dk + B, \quad (41)$$

$$\rho = \sum_{f=u,d} \frac{1}{3} \frac{\gamma_f}{2\pi^2} \int_0^\infty [n_f(k,\mu_f) - n_f(k,-\mu_f)] k^2 dk\,, \quad (42)$$

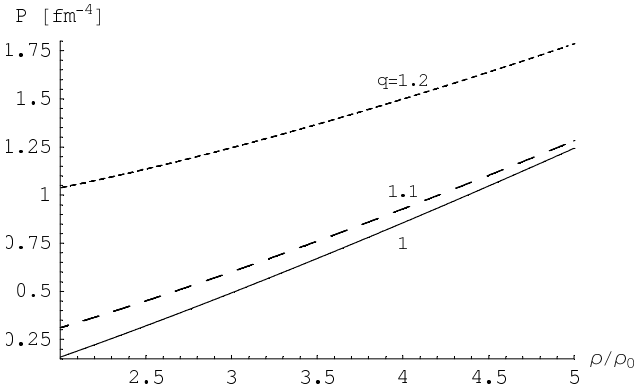

Fig. 7. The same as in Fig. 6 for the case of the quark-gluon equation of state.

where $\epsilon_f = (k^2+m_f^2)^{1/2}$ and $n_f(k,\mu_f)$, $n_f(k,-\mu_f)$ are the particle and antiparticle quark distributions. The quark degeneracy for each flavor is $\gamma_f = 6$. Similar expressions for the pressure and the energy density can be written for the gluons treating them as a massless Bose gas with zero chemical potential and degeneracy factor $\gamma_g = 16$. In this subsection we are limiting our study to the two-flavor case ($f = u,\, d$). As already remarked, this appears rather well justified for the application to heavy ion collisions at relativistic (but not ultra-relativistic) energies, the fraction of strangeness produced at these energies being small [58, 59].

Since one has to employ the fermion (boson) non-extensive distribution (18), the results are not analytical, even in the massless quark approximation. Hence a numerical evaluations of the integrals in Eq.s (40)–(42) must be performed. A similar calculation, only for the quark-gluon phase, was also performed in Ref.[57] by studying the phase transition diagram.

In Fig. 7, we report the EOS for massless quarks u, d and gluons, for different values of q. As in Fig. 6, the results are plotted at the temperature $T = 100$ MeV and at a fixed value of $Z/A = 0.4$; the bag parameter is $B^{1/4}$=170 MeV. In both figures 6 and 7 one can observe sizable effects in the behaviour of the EOS even for small deviations from the standard statistics (the largest value of q employed here is 1.2).

6.3 Mixed hadron-quark phase

In this subsection we investigate the hadron-quark phase transition at finite temperature and baryon chemical potential by means of the previous relativistic EOSs. Lattice calculations predict a critical phase transition temperature T_c of about 170 MeV, corresponding to a critical energy density $\epsilon_c \approx 1$ GeV/fm^3 [1]. In a theory with only gluons and no quarks, the transition turns out to be of first order. In nature, since the u and d quarks have a small mass, while the strange quark has a somewhat larger mass, the phase transition is predicted to be a smooth cross over. However, since it occurs over a very narrow range of temperatures, the transition, for several practical purposes, can still be considered of first order. Indeed the lattice data with 2 or 3 dynamical flavours are not precise enough to unambigously control the difference between the two situations. Thus, by considering the deconfinement transition at finite density as a the first order one, a mixed phase can be formed, which is typically described using the two separate equations of state, one for the hadronic and one for the quark phase.

To describe the mixed phase we use the Gibbs formalism, which in Ref. [60] has been applied to systems where more than one conserved charge is present. In this contribution we are studying the formation of a mixed phase in which both baryon number and isospin charge are preserved. The main result of this formalism is that, at variance with the so-called Maxwell construction, the pressure in the mixed phase is not constant and therefore the nuclear incompressibility does not vanish. It is important to notice that from the viewpoint of Ehrenfest's definition, a phase transition with two conserved charges is considered, in the literature, not of first, but of second order [61].

The structure of the mixed phase is obtained by imposing the Gibbs conditions for chemical potentials and pressure and by requiring the global conservation of the total baryon (B) and isospin densities (I) in the hadronic phase (H) and in the quark phase (Q)

$$\begin{aligned}
&\mu_B^{(H)} = \mu_B^{(Q)}\,,\\
&\mu_I^{(H)} = \mu_I^{(Q)}\,,\\
&P^{(H)}(T,\mu_{B,I}^{(H)}) = P^{(Q)}(T,\mu_{B,I}^{(Q)})\,,\\
&\rho_B = (1-\chi)\rho_B^H + \chi\rho_B^Q\,,\\
&\rho_I = (1-\chi)\rho_I^H + \chi\rho_I^Q\,.
\end{aligned} \tag{43}$$

where χ is the fraction of quark matter in the mixed phase. In this way we can obtain the binodal surface which gives the phase coexistence region in the (T,ρ_B,ρ_I) space. For a fixed value of the conserved charge ρ_I, related to the proton fraction $Z/A \equiv (1+\rho_I/\rho_B)/2$, we study the boundaries of the mixed phase region in the (T,ρ_B) plane. We are particularly interested in the lower baryon density border, i.e. the critical/transition density ρ_{cr}, in order to check the possibility of reaching such (T,ρ_{cr},ρ_I) conditions in a transient state during a heavy-ion collision at relativistic energies.

In Fig. 8, we report the pressure versus baryon number density (in unit of the nuclear saturation density ρ_0) and, in Fig. 9, the pressure as function of the energy density in the mixed hadron-quark phase for different values of q. For the hadronic phase we have used the so-called GM2 set of parameters [54] and in the quark phase the bag parameter is fixed to $B^{1/4}$=170 MeV. The temperature is fixed at $T = 60$ MeV and the proton fraction at Z/A=0.4, physical values which are estimated to be realistic for high energy heavy-ion collisions. The mixed hadron-quark phase starts at $\rho = 3.75\,\rho_0$ for $q = 1$, at $\rho = 3.31\,\rho_0$ for $q = 1.05$ and at $\rho = 2.72\,\rho_0$ for $q = 1.1$. It is important to observe that for $q = 1.1$ it is also reached the second critical transition

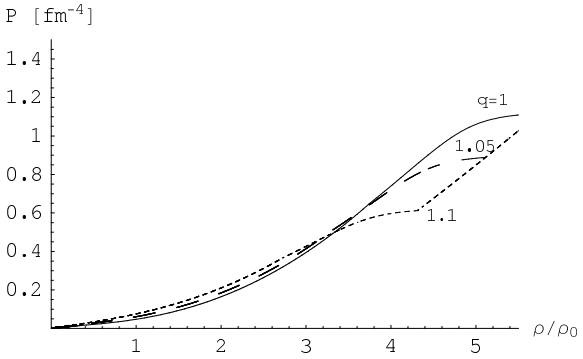

Fig. 8. Pressure versus baryon density in units of the nuclear saturation density ρ_0 in the mixed hadron-quark phase for different values of q. Note that for $q = 1.1$ the second transition density, separating the mixed phase from the pure quark-gluon matter, is reached.

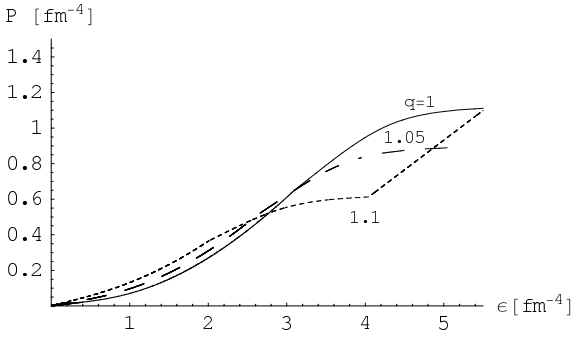

Fig. 9. Pressure versus energy density in the mixed hadron-quark phase for different values of q. As in the previous figure, we note that for $q = 1.1$ the second phase transition to a pure quark-gluon matter is reached.

density, separating the mixed phase from the pure quark-gluon matter phase, at $\rho = 4.29\,\rho_0$ while for $q = 1.05$ the second critical density is reached at $\rho = 5.0\,\rho_0$ and at $\rho = 5.57\,\rho_0$ for $q = 1$.

As a concluding remark we note that non-extensive statistical effects become extremely relevant at large baryon density and energy density, as the ones which can be reached in high energy collisions experiments. This fact can be an important ingredient in the realization of a hydrodynamic model as well as to obtain a deeper microscopic connection with the experimental observables.

References

1. R.C. Hwa, X.N. Wang, *Quark Gluon Plasma 3*, (World Scientific, 2004).
2. T.S. Biró, J. Phys. G: Nucl. Part. Phys. **35** (2008) 044056.
3. S. Ichimaru, Rev. Mod. Phys. **54** (1982) 1017.
4. W.M. Alberico, A. Lavagno, P. Quarati, Eur. Phys. J. C **12** (2000) 499; W.M. Alberico, A. Lavagno, P. Quarati, Nucl. Phys. A **680** (2001) 94c.
5. A. Peshier, W. Cassing, Phys. Rev. Lett. **94** (2005) 172301.
6. M.H. Thoma, J. Phys. G **31** (2005) L7.
7. C. Tsallis, J. Stat. Phys. **52** (1988) 479.
   See also http://tsallis.cat.cbpf.br/biblio.htm for a regularly updated bibliography on the subject.
8. C. Tsallis, R.S. Mendes and A.R. Plastino, Physica A **261** (1998) 534.
9. M. Gell-Mann and C. Tsallis (Editors), *Non-extensive Entropy: Interdisciplinary Applications*, (Oxford University Press, USA, 2004).
10. G. Wilk, Z. Włodarczyk, Phys. Rev. Lett. **84** (2000) 2770; O.V. Utyuzh, G. Wilk, Z. Włodarczyk, J. Phys. G **26** (2000) L39; F.S. Navarra, O.V. Utyuzh, G. Wilk, Z. Włodarczyk, Phys. Rev. D **67** (2003) 114002.
11. G. Kaniadakis, A. Lavagno, P. Quarati, Phys. Lett. B **369**, (1996) 308; A. Lavagno, P. Quarati, Phys. Lett. B **498**, (2001) 47; A. Lavagno, P. Quarati, Nucl. Phys. B [PS] **87** (2000) 209.
12. D.B. Walton, J. Rafelski, Phys. Rev. Lett. **84** (2000) 31.
13. I. Bediaga, E.M.F. Curado, J.M. de Miranda, Physica A **286** (2000) 156.
14. C. Beck, Physica A **286** (2000) 164; Physica A **305** (2002) 209; Physica A **331** (2004) 173.
15. T.S. Biró, G. Purcsel, Phys. Rev. Lett. **95** (2005) 162302.
16. T.S. Biró, B. Müller, Phys. Lett. B **578** (2004) 78; T.S. Biró, A. Peshier, Phys. Lett. B **632** (2006) 247.
17. T.S. Biró, G. Purcsel, Phys. Lett. A **372** (2008) 1174.
18. N. Biyajima, M. Kaneyama, T. Mizoguchi, G. Wilk, Eur. Phys. J. C **40** (2005) 243; N. Biyajima et al., Eur. Phys. J. C **48** (2006) 597.
19. T. Osada, G. Wilk, Phys. Rev. C **77** (2008) 044903.
20. A. Lavagno, Physica A **305** (2002) 238.
21. A. Lavagno, Phys. Lett. A **301** (2002) 13.
22. S.R. Groot, W.A. van Leeuwen, Ch. G. van Weert, *Relativistic kinetic theory*, North-Holland, Amsterdam, 1980.
23. See, for example: C. R. Allton, S. Ejiri, S. J. Hands, O. Kaczmarek, F. Karsch, E. Laermann and C. Schmidt, Phys. Rev. D **68** (2003) 014507.
24. U. Tirnakli, F. Büyükkiliç, D. Demirhan, Phys. Lett. A **245** (1998) 62.
25. I.G. Bearden et al. (BRAHMS Collaboration), Phys. Rev. Lett. **93** (2004) 102301.
26. H. Appelshäuser et al. (NA49 Collaboration), Phys. Rev. Lett. **82** (1999) 2471.
27. L. Ahle et al. (E802 Collaboration), Phys. Rev. C **60** (1999) 064901; J. Barette et al. (E977 Collaboration), Phys. Rev. C **62** (2000) 024901.
28. M. Biyajima et al., Prog. Theor. Phys. Suppl. **153** (2004) 344.
29. T. Csörgö, S. Hegyi, W.A. Zajc, Eur. Phys. J. C **36** (2004) 67.
30. G. Wolschin, Phys. Rev. C **69** (2004) 024906; Europhys. Lett. **74** (2006) 29.
31. R. Kuiper, G. Wolschin, Annalen Phys. **16** (2007) 67.

32. G. Wolschin, M. Biyajima, T. Mizoguchi, Eur. Phys. J. A **36** (2008) 111; G. Wolschin, Ann. Physik **17** (2008) 462.
33. W.M. Alberico, P. Czerski, A. Lavagno, M. Nardi, V. Somá, Physica A **387** (2008) 467.
34. C. Tsallis, D.J. Bukman, Phys. Rev. E **54** (1996) R2197.
35. R. Metzler, J. Klafter, Phys. Rep. **339** (2000) 1.
36. E.K. Lenzi, R.S. Mendes, C. Tsallis, Phys. Rev. E **67** (2003) 031104.
37. M. Csanád, T. Csörgö, M. Nagy, Braz. J. Phys. **37** 3A (2007) 1002.
38. I.G. Bearden et al. (NA44 Collab.), Phys. Rev. Lett. **78** (1997) 2080.
39. M.M. Aggarwal et al. (WA98 Collab.), Eur. Phys. J. C **23** (2002) 225.
40. S.S. Adler et al. (PHENIX Collab.), Phys. Rev. Lett. **91** (2003) 072301; K. Reygers (PHENIX Collab.), Nucl. Phys. A **734** (2004) 74.
41. T. Alber et al. (NA35 Collab.), Eur. Phys. J. C **2** (1998) 643.
42. M. Gaździcki and St. Mrówczyński, Z. Phys. C **54** (1992) 127.
43. St. Mrówczyński, Phys. Lett. B **439** (1998) 6.
44. A. Appelshäuser et al. (NA49 Collab.), Phys. Lett. B **467** (1999) 21.
45. O.V. Utyuzh, G. Wilk, Z. Włodarczyk, Phys. Rev. C **64** (2001) 027901.
46. M. Rybczyński, Z. Włodarczyk, G. Wilk, Acta Physica Pol. B **35** (2004) 819.
47. H. Stoecker, Nucl. Phys. A **750** (2005) 121; M. Isse et al., Phys. Rev. C **72** (2005) 064908.
48. L. Bonanno, A. Drago, A. Lavagno, Phys. Rev. Lett. **99** (2007) 242301.
49. V. N. Russkikh and Y. B. Ivanov, Phys. Rev. C **74**, (2006) 034904.
50. M. Di Toro, A. Drago, T. Gaitanos, V. Greco, A. Lavagno, Nucl. Phys. A **775** (2006) 102; A. Drago, A. Lavagno, I. Parenti, Ap. J. **659** (2007) 1519.
51. A. Drago, A. Lavagno, P. Quarati, Physica A **344** (2004) 472.
52. F.I.M. Pereira, R. Silva, J.S. Alcaniz, Phys. Rev. C **76**, (2007) 015201.
53. P. Senger, J. Phys. G **30** (2004) S1087.
54. N.K. Glendenning, S.A. Moszkowski, Phys. Rev. Lett. **67** (1991) 2414.
55. GSI, Scientific Report 2007 and GSI Proposal for an International Accelerator Facility for Research with Ions and Antiprotons.
56. A. Chodos et al., Phys. Rev. D **9** (1974) 3471.
57. A. Teweldeberhan, H.G. Miller, R. Tegen, Int. J. Mod. Phys. E **12** (2003) 395.
58. G. Ferini, M. Colonna, T. Gaitanos, M. Di Toro, Nucl. Phys. A **762** (2005) 147.
59. C. Fuchs, Prog. Part. Nucl. Phys. **56** (2006) 1.
60. N. K. Glendenning, Phys. Rev. D **46** (1992) 1274.
61. H. Müller and B. D. Serot, Phys. Rev. C **52** (1995) 2072.